AIP | The Journal of Chemical Physics

Calculating energy levels of isomerizing tetra-atomic molecules. I. The rovibrational bound states of Ar 2 HF

Igor N. Kozin, Mark M. Law, Jeremy M. Hutson, and Jonathan Tennyson

Citation: The Journal of Chemical Physics **118**, 4896 (2003); doi: 10.1063/1.1545109
View online: http://dx.doi.org/10.1063/1.1545109
View Table of Contents: http://scitation.aip.org/content/aip/journal/jcp/118/11?ver=pdfcov
Published by the AIP Publishing

Calculating energy levels of isomerizing tetra-atomic molecules. I. The rovibrational bound states of Ar_2HF

Igor N. Kozin and Mark M. Law
Department of Chemistry, University of Aberdeen, Meston Walk, Aberdeen AB24 3UE, United Kingdom

Jeremy M. Hutson
Department of Chemistry, University of Durham, South Road, Durham, DH1 3LE, United Kingdom

Jonathan Tennyson
Department of Physics and Astronomy, University College London, London WC1E 6BT, United Kingdom

(Received 1 November 2002; accepted 18 December 2002)

A general, six-dimensional computational method for the accurate calculation of rotationally and vibrationally excited states of tetra-atomic molecules is developed. The resulting program is particularly appropriate for molecules executing wide-amplitude motions and isomerizations. An application to the Ar_2HF van der Waals trimer is presented in which the HF intramolecular stretching coordinate is separated out adiabatically and is not treated explicitly. Vibrational term values up to about 100 cm^{-1} with absolute convergence to better than 0.1 cm^{-1} are reported. These calculations employ more extensive vibrational basis sets and hence consider a much higher density of states than hitherto. States that sample Ar–Ar–HF linear configurations and approach Ar–HF–Ar linear configurations are characterized for the first time. Results for total angular momentum $J=0$ and 1 provide the first accurate calculations of rotational constants for this system. The rotational constants for the HF bending states of Ar_2HF in the ground and first vibrationally excited states of the HF monomer are in good agreement with experiment, confirming the accuracy of the potential used in this work. © *2003 American Institute of Physics.* [DOI: 10.1063/1.1545109]

I. INTRODUCTION

Recent interest in understanding wide-amplitude (floppy) molecular motions has been stimulated by the drive to develop theories of intermolecular forces, isomerization and coherent control of chemical reactions. Methods for calculating the rotation–vibration energy levels and wave functions of floppy systems have advanced greatly in the last decade but remain technically demanding and computationally expensive even for molecules and complexes as small as tetra-atomics.[1–8]

The accurate calculation of the (ro-)vibrational bound states of the Ar_2HF van der Waals complex is particularly challenging. As well as possessing five floppy (intermolecular) vibrational modes, two linear structures (Ar–Ar–HF and Ar–HF–Ar) are accessible at modest levels of excitation. Both of these local minima lie about 75 cm^{-1} above the T-shaped global minimum structure. Successful solution of this bound-state problem is vital to maximize the understanding of the spectroscopy of this important prototype system for the development of the theory of nonadditive (three-body) intermolecular forces.[9–16]

The Ar_2HF complex is ideally suited for the investigation of nonadditive forces in systems involving a molecular constituent. The Ar_2 and ArHF pair potentials are very accurately known, having been determined by accurate fitting to experimental data by Aziz[17] and Hutson,[18] respectively. Moreover there is a high-quality experimental data set available that is sensitive to the three-body part of the intermolecular potential. The experimental data include microwave,[19] mid-infrared[9,13,20] and near-infrared[15] spectroscopic observations. Investigations of the nonadditive forces in the Ar_2HF complex using *ab initio* electronic structure calculations have included the applications of supermolecular Møller–Plesset perturbation theory by Szczęśniak, Chałasinski, and co-workers[10,11] and symmetry-adapted perturbation theory by Moszynski and co-workers.[16]

Hutson and co-workers[2,12,14,21–23] have developed and tested a model of the nonadditive forces in Ar_2HX (where X = halogen) including dispersion, induction, exchange overlap and exchange multipole interactions. Ernesti and Hutson[14] found that their total-1 model (referred to hereafter as the EH potential) reproduced well the vibrational band origins and frequency shifts for Ar_2HF, Ar_2DF, Ar_2HCl, and Ar_2DCl in the H/DX $v=0$ and 1 states. The model has also been extended to Ar_nHF clusters[24] and shown to reproduce the observed vibrational shifts for $n=3$ and 4. However, the bound-state calculations of Ernesti and Hutson for Ar_2HF were restricted to total angular momentum $J=0$. The rotational constants were computed as expectation values based on pure vibrational wave functions and hence did not include Coriolis terms which are very large in some cases. Thus detailed comparisons of the predictions based on Ernesti and Hutson's nonadditive potentials with observed rotational constants have not been possible hitherto. One important objective of the present work is to address this issue by computing rotationally excited ($J>0$) bound states of the Ar_2HF complex.

Ernesti and Hutson's bound-state variational calculations employed diatom–diatom (Jacobi) coordinates and a near-

exact kinetic energy operator to describe the internal motion of the Ar_2HX complexes. The complete 5D intermolecular potential was averaged over the vibrational motion of HX in the adiabatically decoupled vibrational state v_{HF}. The basis set was carefully optimized to converge well the ground van der Waals states and the fundamental HX bending excitations (for each v_{HF}). However, the basis set was restricted to configurations associated with the T-shaped (global) minimum.

Continuing advances in computing power and recent important developments in methodology for dealing with floppy systems make it now feasible to compute bound-state energies and wave functions of tetra-atomic molecules which probe multiple minima and include rotational excitation. However, as far as we are aware there has been only one reported study of variational calculations on a rotationally excited system with as many as five floppy vibrational modes.[25] Most recently Lee and McCoy[7] have computed variationally the 25 lowest vibrational ($J=0$) states of the Ne_2SH and Ne_2OH ($\tilde{A}\,^2\Sigma^+$) complexes. These authors characterized T-shaped and linear ''isomers'' with geometries analogous to those expected to be accessible in Ar_2HF.

In the light of these developments it is timely to extend the theoretical study of the Ar_2HF complex to include characterization of vibrational states associated with the linear isomers. To date no spectroscopic observations of such states have been made (nor indeed of any of the ''framework modes'' associated with heavy-atom vibrations about the T-shaped configuration). Nevertheless there are excited states with these characteristics that lie close in energy to the states that have been observed, and perturbations due to them could well be important.

The structure of the remainder of this paper is as follows: Section II describes the theoretical methods that we have developed and implemented to calculate the bound states of floppy tetra-atomic systems. Section III outlines the results for the pure vibrational ($J=0$) states of Ar_2HF. This includes discussion of the global picture of vibrational states involving all three local minima. The detailed investigation of the rotationally excited HF bending vibrational states of Ar_2HF and the implications for the EH potential are discussed in Sec. IV. Section V concludes the paper.

II. COMPUTATIONAL METHOD

Coordinates based on orthogonal vectors have become a very popular choice in dealing with wide-amplitude motions in polyatomic systems. The generalized approach used in this work was suggested by Chapuisat and Iung[1] and developed further in Refs. 26 and 27. Recently Mladenović gave a very concise account of the approach together with a detailed description of applications to some molecules.[5] Fundamentally we build on the results of Ref. 5, although computationally our method is somewhat different.

One of the most attractive features of generalized orthogonal coordinates is the simplicity of the kinetic energy operator,

$$T=\sum_{\alpha=1}^{3} -\frac{\hbar^2}{2\mu_\alpha}\left(\frac{\partial^2}{\partial q_\alpha^2}+\frac{2}{q_\alpha}\frac{\partial}{\partial q_\alpha}\right)+T_{\mathrm{ang}}, \tag{1}$$

where μ_α are reduced masses, q_α are the lengths of internal vectors $\mathbf{q}_\alpha$ and T_{ang} is the angular kinetic operator given in Eq. (37) of Ref. 5. Perhaps even more important is the invariance of Eq. (1) under various choices of orthogonal vectors. Several useful choices such as Radau, Jacobi, diatom–diatom and orthogonal satellite vectors are considered in Refs. 3 and 5. Once the scheme is chosen, the body-fixed axis system is usually defined so that the z axis goes along one of the vectors, for example, $\mathbf{q}_3$, and the xz plane is defined by $\mathbf{q}_3$ and $\mathbf{q}_1$.

The disadvantage of Eq. (1) is that potentially it has two types of singularities, both of which are connected with T_{ang}. One singularity corresponds to the angle between $\mathbf{q}_3$ and $\mathbf{q}_1$ being zero or π (so that the molecular plane is not defined). This can be cured by using a nondirect product angular basis[28]—for a recent general discussion see, for example, Ref. 29. Another singularity arises when q_3 is equal to zero (so that the z axis is not defined). Unfortunately, depending on the choice of coordinates, one or both of these singularities is physically accessible for many floppy four-atom molecules. To deal with the latter type of singularity we have employed spherical oscillator functions.[30]

Our treatment of the angular problem is essentially close to that of Mladenović,[5] who gave the matrix elements of T_{ang} in a parity-adapted angular basis. Unfortunately, the equations for the matrix elements in Ref. 5 contain two typographical errors. In addition, we have found it more convenient to work with slightly different phase factors for the angular basis. We therefore present the matrix elements below. Our primitive angular basis functions are

$$|\kappa Kkjl,Jp\rangle = N_{Kk}\kappa^k P_j^{|k-\kappa K|}[Y_l^{\kappa k}|J,K,M\rangle + (-1)^{J+p+K+k}Y_l^{-\kappa k}|J,-K,M\rangle], \tag{2}$$

where κ is an auxiliary number taking the values -1 and $+1$, J and K are the usual rotational quantum numbers associated with the total angular momentum and its projection on the body-fixed z-axis, j and l are angular momenta associated with rotation of $\mathbf{q}_1$ and $\mathbf{q}_2$, respectively, k is the projection of l onto $\mathbf{q}_3$, p is the total parity, N_{Kk} is a normalization factor, P_j^k are associated Legendre functions of the angle between $\mathbf{q}_3$ and $\mathbf{q}_1$, Y_j^k are spherical harmonics of the body-fixed angles defining the direction of $\mathbf{q}_2$ and $|J,K,M\rangle$ are symmetric top eigenfunctions. When $\kappa=1$ our angular basis functions are the same as in Ref. 5, but they differ by a factor $(-1)^{J+p+K}$ when $\kappa=-1$.

It is useful to introduce radial functions

$$b_1=\frac{\hbar^2}{2\mu_1 q_1^2}+\frac{\hbar^2}{2\mu_3 q_3^2}, \tag{3}$$

$$b_2=\frac{\hbar^2}{2\mu_2 q_2^2}+\frac{\hbar^2}{2\mu_3 q_3^2}, \tag{4}$$

$$b_3=\frac{\hbar^2}{2\mu_3 q_3^2}. \tag{5}$$

J and p are strictly conserved and are therefore omitted in the formula below.

The matrix elements diagonal in K are given by

$$\langle \kappa,K,k,j,l|T_{\rm ang}|\kappa,K,k,j,l\rangle = b_1 j(j+1)+b_2 l(l+1)+b_3[J(J+1) -2(K^2+k^2-\kappa Kk)], \quad (6)$$

$$\langle \kappa,K,k',j,l|T_{\rm ang}|\kappa,K,k,j,l\rangle = b_3\,\mathrm{sign}(k-\kappa K)\sqrt{1+\delta_{K0}\delta_{k0}}C^{+}_{j,k-\kappa K}C^{+}_{l,k}\delta_{k',k+1} + b_3\,\mathrm{sign}(k'-\kappa K)\sqrt{1+\delta_{K0}\delta_{k1}}C^{-}_{j,k-\kappa K}C^{-}_{l,k}\delta_{k',k-1}, \quad (7)$$

$$\langle \kappa'=1,K,k'=1,j,l|T_{\rm ang}|\kappa=-1,K,k=0,j,l\rangle = -b_3 C^{-}_{j,K}C^{-}_{l,0}, \quad (8)$$

where $C^{\pm}_{lk}=\sqrt{l(l+1)-k(k\pm1)}$. The quantity sign($I$) takes the value -1 if $I<0$ and $+1$ if $I\geqslant 0$. Inspection shows that these matrix elements do not depend on the parity quantum number p. This allows the eigenvectors for the $K>0$ diagonal blocks to be reused in the construction of the matrix elements for the off-diagonal blocks (see below).

The matrix elements off-diagonal in K are given by

$$\langle \kappa,K'=K-1,k',j,l|T_{\rm ang}|\kappa,K,k,j,l\rangle = -\kappa b_3 C^{-}_{JK}[C^{-\mathrm{sign}(\kappa)}_{l,k}\delta_{k',k-\kappa}+\mathrm{sign}(k-\kappa K) \times\sqrt{1+\delta_{K1}\delta_{k0}}C^{\mathrm{sign}(\kappa)}_{j,k-\kappa K}\delta_{k',k}], \quad (9)$$

$$\langle \kappa,K'=K+1,k',j,l|T_{\rm ang}|\kappa,K,k,j,l\rangle = -\kappa b_3 C^{+}_{JK}[C^{\mathrm{sign}(\kappa)}_{l,k}\delta_{k',k+\kappa}+\mathrm{sign}(k-\kappa K') \times\sqrt{1+\delta_{K0}\delta_{k0}}C^{-\mathrm{sign}(\kappa)}_{j,k-\kappa K}\delta_{k',k}], \quad (10)$$

$$\langle \kappa'=1,K=1,k,j,l|T_{\rm ang}|\kappa=-1,K=0,k,j,l\rangle = -b_3 C^{+}_{J,0}C^{-}_{j,k}(-1)^{J+p}, \quad (11)$$

$$\langle \kappa'=1,K=1,k+1,j,l|T_{\rm ang}|\kappa=-1,K=0,k,j,l\rangle = -b_3\sqrt{1+\delta_{k0}}C^{+}_{J,0}C^{+}_{l,k}(-1)^{J+p}, \quad (12)$$

$$\langle \kappa'=1,K'=K+1,k'=1,j,l|T_{\rm ang}|\kappa=-1,K,k=0,j,l\rangle = -b_3\sqrt{1+\delta_{K0}}C^{+}_{J,K}C^{+}_{l,0}. \quad (13)$$

If $K=k=0$ and $J+p$ is even then the last two equations are the same and need be used only once.

The program suite[31] developed to perform the present study is capable of full six-dimensional (6D) rovibrational calculations and has no limitation on the choice of orthogonal vectors. After some consideration, we decided to use diatom–diatom vectors for the application to Ar_2HF. The Ernesti and Hutson total-1 Ar_2HF potential[14] was constructed using these coordinates. The potential was explicitly constructed so that HF vibrations are adiabatically separated and therefore each $v_{\rm HF}$ state is treated separately. This effectively corresponds to averaging of $q_2=r_{\rm HF}$ (to reproduce correctly the HF rotational constant for each $v_{\rm HF}$) in Eq. (1) and reducing the number of degrees of freedom by one. The present diatom–diatom coordinates are almost identical to the ones used in Ref. 14 if one takes the Ar–Ar distance $\rho=q_1$ and the distance between the centers of mass of the two diatoms $R=q_3$; see the diagram in Fig. 1. The only essential difference is in the axes embedding. The vector $\mathbf{q}_3$ defines the direction of the z axis and together with $\mathbf{q}_1$ defines the xz plane. θ_1 is the angle between the two vectors. The orientation of vector $\mathbf{q}_2$ is given by two angles θ_2 and ϕ; the angle between $\mathbf{q}_2$ and $\mathbf{q}_3$ is θ_2 and ϕ rotates $\mathbf{q}_2$ around $\mathbf{q}_3$. The angular momentum of Ar_2 is denoted $j_{\mathrm{Ar}_2}=j$ and that of HF is denoted $j_{\rm HF}=l$ here, while k is the projection of $j_{\rm HF}$ onto R. Note, however, that in most of the earlier literature it was $j_{\rm HF}$ that was denoted by j.[12,14] Note also that θ_1 and θ_2 here correspond to $\pi-\chi$ and $\pi-\theta$ respectively in Ref. 2 but χ and $\pi-\theta$ respectively in Ref. 12.

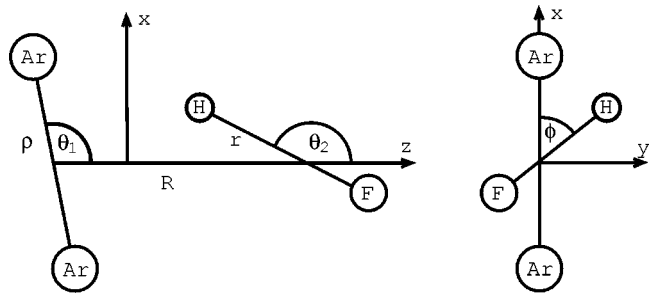

FIG. 1. Coordinate system used for Ar_2HF.

A major advantage of Eq. (1) is that it helps separate radial and angular coordinates because no mixed derivative angular–radial operators are present. Thus if the radial motion is treated in the discrete variable representation (DVR)[32,33] the whole problem can be effectively constructed from a set of angular subproblems. Furthermore the use of the DVR approximation for the potential energy requires only the angular integrals to be computed explicitly. Two possible radial basis functions have been considered in the present work: Morse oscillatorlike functions and spherical oscillator functions. Morse oscillatorlike functions are defined as[34]

$$\beta^{1/2}N_{n\alpha}\exp(-y/2)y^{(\alpha+1)/2}L^{\alpha}_{n}(y), \quad (14)$$

where $y=\alpha\exp[-\beta(r-r_e)]$, $\alpha=4D_e/\beta$, $\beta=\omega_e(\mu/2D_e)^{1/2}$, $L^{\alpha}_{n}(y)$ is a Laguerre polynomial, μ is the reduced mass associated with radial distance r and $N_{n\alpha}$ is a normalization factor. The set $\{r_e,\ \omega_e,\ D_e\}$ are treated as parameters to be optimized, although they can be associated with the equilibrium distance, fundamental frequency and dissociation energy. In the case where the distance r can be zero, spherical oscillator functions[30] are a better choice,

$$\sqrt{2}\beta^{1/4}N_{n\,\eta+1/2}\exp(-y/2)y^{(\eta+1)/2}L^{\eta+1/2}_{n}(y), \quad (15)$$

where $y=\beta r^2$, $\beta=(\mu\omega_e)^{1/2}$ and $\{\eta,\ \omega_e\}$ are treated as parameters.

The size of the primitive basis is necessarily very big. If we had a pure DVR basis, we could use methods which do not require explicit storage of the Hamiltonian matrix for finding eigenvectors. Unfortunately the nondirect product part of our basis cannot be transformed effectively to a DVR and so integration of the angular potential function must be performed. Recently Lee and McCoy[7] had a similar problem.

They decided to use the implicit sequential diagonalization and truncation approach.[35] In the present work we use more traditional explicit sequential diagonalization and truncation (see, for example, Ref. 33). The computation is performed in several steps. First the angular kinetic energy operator is separated into sub-blocks diagonal in K, $T^K_{\rm ang}$, and sub-blocks off-diagonal in K with $\Delta K=\pm 1$, $T^{K',K}_{\rm ang}$. The angular problem associated with $T^K_{\rm ang}+V$ is solved separately for every K sub-block for all radial grid point pairs (R,ρ). Here V is the full five-dimensional (5D) potential with fixed R and ρ. Only eigenfunctions below a certain energy cutoff, $E^{(1)}_{\rm cut}$ are selected for later use. Then the kinetic energy operator in the radial coordinate ρ is included and the respective matrices are constructed in the angular plus ρ basis and solved for eigenvectors for every R point. Again only the lowest states, this time below $E^{(2)}_{\rm cut}$, are selected. Then the kinetic energy operator in R is included and the full 5D vibrational matrix is computed. During this step only the eigenvalues below $E^{(3)}_{\rm cut}$ are found. For $K=0$ this gives the desired final vibrational levels. For $K>0$ it gives K-optimized eigenvectors for further use in the final ro-vibrational step. As outlined above, the contracted eigenvectors for $p=0$ and $p=1$ are identical for the $K>0$ diagonal sub-blocks. Hence the contracted eigenvectors for $p=0$ can be used for both $p=0$ and $p=1$ in the final step. In this final step, $\Delta K=\pm 1$ sub-blocks are included and rovibrational levels are computed.

Depending on the size of the angular basis, the computation of the three-dimensional angular integrals of the potential function may be the most time-consuming part of the calculation. Therefore it is important to make it as efficient as possible. To facilitate this in the present case we have tried expanding the potential in the $J=0$, totally symmetric angular functions defined by Eq. (2) at every radial pair and computing the angular integrals analytically. This allowed reusing the expansion for all symmetries. We found that this strategy is useful when particularly accurate integrals are desired. However for Ar_2HF the best ratio of performance to accuracy was found with direct integration of the potential function using Gaussian quadrature on the minimal number of quadrature points. This was achieved after implementing an algorithm which takes into account the symmetry properties of the product of two primitive basis functions. The summation is performed only over half of the quadrature points but it uses the symmetric part of the potential if the product is symmetric and the asymmetric part if the product is asymmetric. In choosing the number of quadrature points, we used the minimum number of points required to maintain the orthogonality of the basis functions. These numbers are $j^{\rm max}_{\rm HF}+1$, $k^{\rm max}+1$, and $j^{\rm max}_{\rm Ar_2}+1$. Normally one would use $2j^{\rm max}_{\rm HF}+1$, $2k^{\rm max}+1$, and $2j^{\rm max}_{\rm Ar_2}+1$ points, respectively. So the approximately twofold saving for every angular coordinate gave an almost eightfold overall saving. This trick has been used previously in expanding a function in a series of spherical harmonics.[36] Furthermore, there is an additional twofold saving for ϕ. Although ϕ is defined from zero to 2π, because of the inversion symmetry its effective range is from zero to π only.

To make further improvements one can compute only once the integrals between different k for all θ_1 and θ_2 grid points and then reuse them in computing 2D integrals.[7] In addition to space-fixed inversion, which separates the states of even and odd parity, the permutation of two Ar atoms is also feasible.[12] This symmetry separates blocks with even and odd $j_{\rm Ar_2}$ and therefore has a straightforward effect on the whole matrix.

Ar_2–HF can be considered as a relatively weakly bound trimer in which the HF exhibits hindered rotation. The equilibrium configuration is a near-isosceles triangle ($R=2.9$ Å, $\rho=3.7$ Å), but two linear configurations are also accessible: Ar–Ar–HF and Ar–HF–Ar. For $v_{\rm HF}=0$ they are located at 77 $\rm cm^{-1}$ ($R=5.3$ Å, $\rho=3.7$ Å) and 74 $\rm cm^{-1}$ ($R=0.03$ Å, $\rho=6.8$ Å), respectively, above the absolute minimum. To accommodate these configurations we used 42 Morse oscillatorlike basis functions defined by Eq. (14) $\{r_e=5.2$ Å, $\omega_e=10$ $\rm cm^{-1}$, $D_e=500$ $\rm cm^{-1}\}$ in ρ, sampling the range from 2 to 8 Å, and 48 spherical oscillator functions defined by Eq. (15) $\{\eta=0$ or 1, $\omega_e=10$ $\rm cm^{-1}$, $D_e=500$ $\rm cm^{-1}\}$ in R, sampling the range from 0 to 6 Å. The parameters were chosen so that the Gaussian grid covers all configurations of interest and the eigenvalues of the respective one-dimensional problems (with all other coordinates fixed to their equilibrium values) are reasonably well converged.

There is no problem in treating the Ar–Ar–HF linear configuration in our approach since we use a coupled angular basis. However, the Ar–HF–Ar configuration requires special attention. The problem of the $1/R^2$ singularity is well known in triatomic systems such as H_3^+ and Ar_3 (if treated using Jacobi coordinates for example): the DVR quadrature approximation breaks down for this term in the kinetic energy operator.[37] The reader is referred to an excellent paper[38] which explicitly considered the problem of singularities and implications made by the choice of direct or nondirect product bases. The conclusion of Ref. 38 is that strictly speaking one needs a nondirect product angular–radial basis to account fully for the $1/R^2$ singularity. However frequently a simpler direct product approximation works well.[37,39] This simpler approach involves the use of basis functions with nonzero probability density at $R=0$ if it is allowed by symmetry and basis functions with zero probability density at $R=0$ otherwise. If sampling $R=0$ is important, it will manifest itself in different energy levels computed using the two types of basis functions.

The spherical oscillator functions (15) have nonzero probability density at $R=0$ if $\eta=0$ and zero if $\eta>0$. In fact the Gaussian quadrature points in R never take exactly zero values, but sample the area near it. Therefore we may use $\eta=0$ functions if the symmetry allows nonzero probability density at $R=0$ and $\eta=1$ functions otherwise. In our implementation, there is also an option to compute $1/R^2$ (required in $T_{\rm ang}$) either in the DVR approximation or analytically.[37] The term $1/\rho^2$, also present in $T_{\rm ang}$, is always treated in the DVR approximation, because the potential does not allow geometries around $\rho=0$ to be sampled.

Our calculations showed that changing η from 0 to 1 has almost no effect for levels up to 100 $\rm cm^{-1}$ above the zero-point energy (ZPE). However using $\eta=0$ and computing

$1/R^2$ analytically made the overall convergence of levels much slower and the computation more demanding. This is because of the spectral range of the $1/R^2$ term:[38–40] as R comes close to zero, $1/R^2$ has not only large diagonal matrix elements but also large off-diagonal elements as well. Consequently our diagonalization–truncation strategy becomes less effective: we have to increase the energy cutoff. However increasing it brings in many more states because the density of states is very high at large R. Therefore in the present work we decided to limit attention to vibrational states below 100 cm^{-1}. All the calculations presented here use $\eta=0$ and treat $1/R^2$ in the DVR approximation. All the $J=0$ eigenvalues calculated using this approach agreed within our level of convergence (0.1 cm^{-1}) with results using $\eta=1$ and treating $1/R^2$ analytically. However, some states above 100 cm^{-1} begin to sample $R=0$ (see below) and we plan to treat them more accurately in a future work.

Dissociation along ρ (giving Ar + Ar + HF) requires about 100 cm^{-1} more energy than dissociation along R (giving Ar_2+HF). It therefore seems logical to treat ρ first in our diagonalization truncation scheme. To ensure that proper ρ functions are obtained, we choose $E_{\rm cut}^{(1)}$ to be above the dissociation energy in ρ by 10 to 50 cm^{-1}. The second energy cutoff, $E_{\rm cut}^{(2)}$, was chosen to be above the second dissociation energy (along R) by 60 to 100 cm^{-1}. To construct the angular basis we used $j_{\rm Ar_2}^{\rm max}=52$, $j_{\rm HF}^{\rm max}=5$, and $k^{\rm max}=4$. This resulted in about 500 angular basis functions per symmetry block for $K=0$ and up to about 900 for $K=1$. Typically a full $J=0$ calculation took several hours on a single 667 MHz XP/1000 Alpha processor and $J=1$ took from 10 hours to 2 days depending on the size of the basis (up to 10 000 contracted functions in the final diagonalization).

III. VIBRATIONAL STATES OF Ar_2HF

Solving the angular problem for all radial configurations results in sets of angular eigenstates (adiabats). The energy of the lowest angular state computed for a radial pair (ρ,R) characterizes the accessibility of the radial configuration concerned. It is instructive to consider the effective 2D potential surface formed by the lowest adiabat. Figure 2 shows an example for $v_{\rm HF}=1$, A_1 symmetry. The two linear configurations are readily recognizable at approximately 100 cm^{-1} above the equilibrium and are seen as local minima. However the Ar–Ar–HF configuration is more easily accessible than Ar–HF–Ar because the barrier to it is lower. The density of angular states is very high at the Ar–Ar–HF configuration and in fact is even higher than at the T-shaped configuration because the angular anisotropy is lower.

The $J=0$ levels computed for $v_{\rm HF}=0$ and 1 are presented in Table I. We estimate that they are converged to better than 0.1 cm^{-1}. We investigated increasing the radial and angular primitive bases by about 20%, but it turned out that the most crucial step to improve convergence was to increase the energy cutoffs. Because we were constrained by memory limitations, the computation was necessarily a compromise between truncation energies and the size of the primitive basis. Fortunately DVR makes it easy to skip points with unphysically high potential energies. Thus actually many points, such as very short-range ρ points, were omitted (before the angular diagonalization at that point).

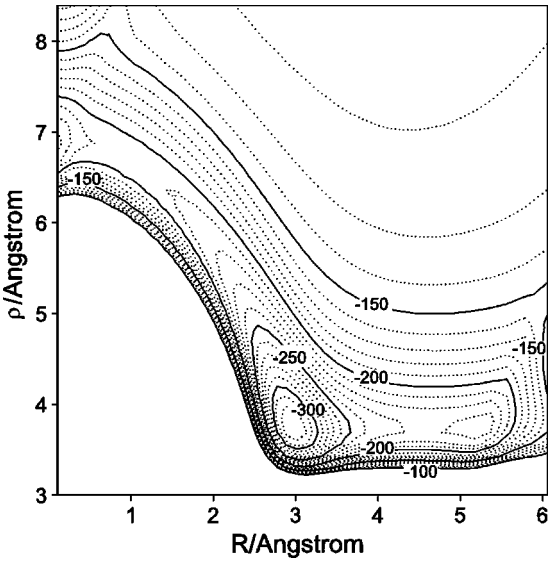

FIG. 2. Effective radial potential energy, constructed using the angular zero-point energy at each radial configuration for $v_{\rm HF}=1$. The contour energies are given in cm^{-1}.

Apart from the ground vibrational state of the complex, so far only HF hindered rotor (or bending) states have been observed experimentally, with $v_{\rm HF}=1$[13] and $v_{\rm HF}=3$.[15] This is because it is the HF rotational motion that carries the oscillator strength for the transitions. Because of the high density of states, it was important to distinguish the HF bending states from the framework modes. This was achieved in two ways. First we computed the relative vibrational line strengths of the transitions from the ground state $v_{\rm HF}=0$ to all computed states

$$RL=\sum_{\alpha=x,y,z}\langle i|\mu_\alpha|f\rangle^2, \tag{16}$$

where i and f denote the initial and final states. Here we have used the approximate dipole moment function given in Ref. 2,

$$\mu_z=\mu_{\rm HF}\sqrt{4\pi/3}\quad Y_1^0, \tag{17}$$

$$\mu_x=\mu_{\rm HF}\sqrt{4\pi/3}\quad (Y_1^{-1}-Y_1^1)\frac{1}{\sqrt{2}}, \tag{18}$$

$$\mu_y=\mu_{\rm HF}\sqrt{4\pi/3}\quad (Y_1^{-1}+Y_1^1)\frac{i}{\sqrt{2}}. \tag{19}$$

It is important to note the selection rules governing the dipole transitions. The operator μ_z transforms as the A_1 representation of the group C_{2v}, so that the only allowed transitions from the ground state are those to states of the same, i.e., A_1, symmetry. Since μ_x is of B_2 symmetry, it allows only transitions to B_2 states. Similarly μ_y allows transitions to B_1 states only. Only relative line strength calculations are presented below, so we take $\mu_{\rm HF}=1$.

In cases where an unambiguous assignment does not emerge from the line strengths, we analyzed the probability

TABLE I. Vibrational energy levels for Ar_2HF ($v_{HF}=0$ and 1) calculated using the EH total-1 potential (Ref. 14). All energies are given in cm^{-1}. ZPE represents zero-point energy. RL represents relative line strength (in units of μ^2_{HF}).

	$v_{HF}=0$		$v_{HF}=1$	
	Energy	RL$\times 10^3$	Energy	RL$\times 10^3$
ZPE	−277.3	−	−291.9	
A_1				
1	0.0	465.56	0.0	488.27
2	25.1	0.04	25.5	0.00
3	39.8	0.20	41.2	0.01
4	46.8	0.01	47.6	0.00
5	56.1	0.03	58.0	0.02
6	62.1	0.02	63.6	0.00
7	66.0	0.05	67.6	0.00
8	70.8	0.26	73.5	0.01
9	71.7	73.64[a]	78.4	0.04
10	76.7	0.00	79.5	48.90[a]
11	78.4	0.78	81.7	9.51
12	81.1	0.01	83.5	0.02
13	83.7	0.09	86.7	0.16
14	85.8	0.02	88.7	0.20
15	86.7	0.02	90.3	0.03
16	87.8	0.00	91.2	0.10
17	88.8	0.11	92.7	0.30
18	90.3	2.16	93.8	3.18
19	91.3	0.03	95.3	0.00
20	92.8	0.00	95.5	0.00
B_2				
1	29.7	7.40	30.5	8.90
2	54.4	0.33	55.7	0.97
3	59.3	123.32[b]	61.1	123.14[b]
4	60.3	104.46[c]	62.2	106.73[c]
5	74.2	0.74	77.1	0.73
6	76.7	0.01	78.2	0.06
7	82.3	1.31	84.1	1.92
8	82.8	0.01	86.2	0.06
9	85.6	0.07	88.1	0.19
10	86.5	0.04	90.7	0.04
11	87.7	0.04	91.9	0.03
12	89.9	0.01	94.0	0.00
13	92.5	0.01	96.4	0.02
B_1				
1	81.6	167.01[d]	87.7	171.99[d]
A_2				
1	107.5		114.3	

[a]Σ bend.
[b]State strongly mixed with in-plane Π bend.
[c]In-plane Π bend (strongly mixed with framework mode).
[d]Out-of-plane Π bend.

density of the computed eigenfunctions. A very useful quantity proved to be the two-dimensional probability density as a function of ρ and R (integrated over the remaining degrees of freedom). Some examples for states of A_1 and B_2 symmetry are given in Figs. 3 and 4. The pure HF bending states have no excitation in radial coordinates and are therefore localized around the absolute minimum in the potential—see, for example, state 10 in Fig. 3. This should be contrasted with states 9 and 11. States 3 and 4 of B_2 symmetry have similar appearance and strong intensity for both $v_{HF}=0$ and 1. In this case the final assignment of the in-plane Π bend (for $v_{HF}=1$) has been made based on the rotational constants (see below).

The present calculations show two strongly interacting B_2 symmetry vibrational states with nearly equal vibrational line strength at about 60 cm^{-1} for Ar_2HF in the $v_{HF}=1$ manifold. These states are separated by only 1 cm^{-1}. Only one band has been identified experimentally.[13] However, the observed band is highly perturbed and only 60% of the resolved lines have been assigned.[13] Some of the unassigned lines might well be attributable to our second predicted vibrational state (at 61.1 cm^{-1}). Before drawing a firm conclusion on this point, however, the approximations associated with our line strength calculations need further investigation. The major approximation is associated with truncation of the basis set: improvements in the basis set may change the relative energies of the two interacting vibrational states and thus change the mixing between them. With a very much smaller basis set, Ernesti and Hutson predicted only one strong vibrational transition to a B_2 state in the region around 60 cm^{-1}.[12,14] The present calculations are definitely more accurate than those of Refs. 12 and 14, but may not be fully converged. In addition, we have so far computed only vibrational rather than rovibrational line strengths, and the latter would be very interesting because they would permit detailed comparison with the experimental data.

The present $J=0$ calculations agree very well with earlier calculations.[12,14] The HF bending states are usually within 0.1 to 0.2 cm^{-1} of the previous results. Comparison of our Table I with Fig. 5 of Ref. 12 immediately demonstrates that many states associated with the framework modes are lower in energy in the present work and the density of states quickly reaches one per cm^{-1}. This is because the work of EH[12,14] was primarily interested in HF bending states and therefore did not use a large enough radial basis set to permit Ar–Ar–HF linear geometries.

In the present work we clearly see that some states probe the Ar–Ar–HF configuration, for example, state 16 in Fig. 3. This state appears to be well localized in the linear isomeric structure. In fact, due to permutation symmetry there is an equivalent state of B_2 symmetry (state 10 in Fig. 4) at about the same energy. States localized in a linear isomeric structure have also been reported in the Ar_3 system.[39]

At yet higher energy, some states begin to sample the Ar–HF–Ar configuration. In this respect it is interesting to compare the radial distribution density for state 20 in Fig. 3 with the wave functions of the ''horseshoe'' states computed for H_3^+ by Tennyson and co-workers[41,42] and for Ar_3 by Wright and Hutson.[39] Here the HF molecule moves between the two Ar atoms as they move apart to make way for it.

As an illustration of the complexity of some of the states arising in this floppy system, state 15 in Fig. 3 shows an irregular nodal structure and samples a very wide range of radial configurations.

IV. ROTATIONALLY EXCITED HF BENDING STATES

The agreement between the vibrational energies computed in this work and those obtained by EH for HF bending states demonstrates that at least some HF bending states are

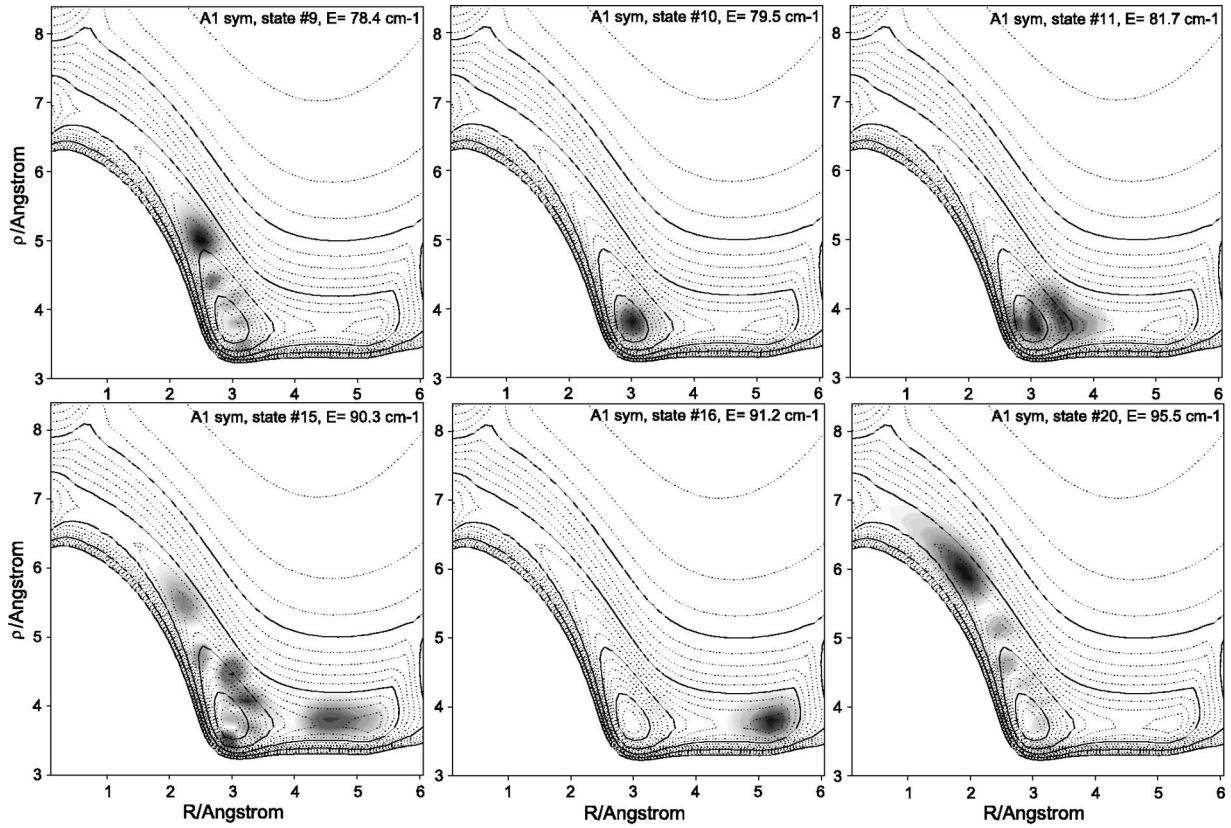

FIG. 3. Probability densities of selected vibrational states for Ar_2HF $v_{HF}=1$, A_1 symmetry calculated using the EH total-1 potential (Ref. 14).

weakly coupled to the framework modes. This encouraged us to try to calculate rotational constants from $J=1$ calculations, despite the lack of absolute convergence in the energies. It seemed reasonable to suppose that if vibrational states are weakly coupled and relatively isolated then rotational spacings might be much better converged than absolute energies.

The rotational excitation from $J=0$ to 1 splits every vibrational level into three rovibrational levels, which have symmetries supplementing the representation of the vibrational state in the full C_{2v} group. For example, if the vibrational state is A_1 then its $J=1$ states will be A_2, B_1, and B_2. Since there is actually just one $J=0$ state of B_1 symmetry below 100 cm^{-1}, and no states of A_2 symmetry, it was easy to match the rovibrational states with the corresponding pure vibrational states. If centrifugal distortion is neglected, the three $J=1$ states have energies $A+B$, $B+C$, and $A+C$ above the corresponding $J=0$ states. This allows the direct computation of the rotational constants *A*, *B*, and *C* from the rovibrational levels. The results are summarized in Table II.

Previous estimates of rotational constants in Ar_2HF have been obtained through calculations of expectation values involving pure vibrational wave functions.[12,14] This neglects Coriolis effects. When the EH calculations and experiment agree, indicating that the Coriolis effects are small or unim-

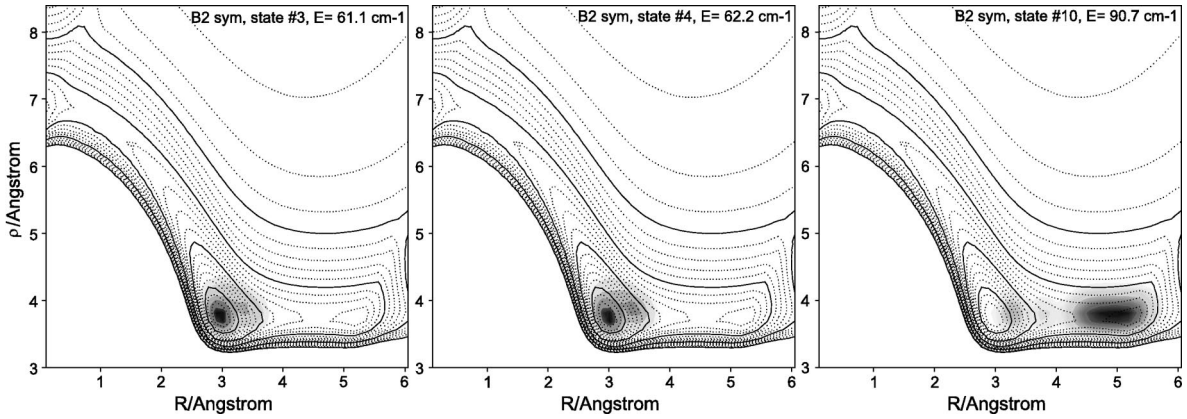

FIG. 4. Probability densities of selected vibrational states for Ar_2HF $v_{HF}=1$, B_2 symmetry calculated using the EH total-1 potential (Ref. 14).

TABLE II. Observed and calculated vibrational energies (cm^{-1}) and rotational constants (MHz) for the van der Waals ground states and HF bending states of Ar_2HF.

	Expt.[a]	EH[b]	Expt.–EH	TW[c]	Expt.–TW
	$v_{HF}=0$, ground state			(A_1 state No. 1)	
A	3576.5	3593.7	−17.2	3578.1	−1.6
B	1739.2	1740.0	−0.8	1740.1	−1.0
C	1160.9	1160.5	0.4	1165.9	−4.9
	$v_{HF}=0$, Σ bend			(A_1 state No. 9)	
ν		71.8		71.7	
A		3553.7		3437.5	
B		1743.4		1745.2	
C		1156.4		1180.4	
	$v_{HF}=0$[d]			(B_2 state No. 3)	
ν				59.3	
A				3450.0	
B				1734.5	
C				1137.4	
	$v_{HF}=0$, in-plane Π bend[e]			(B_2 state No. 4)	
ν		60.1		60.3	
A		3642.3		3365.3	
B		1718.2		1740.0	
C		1154.8		1126.2	
	$v_{HF}=0$, out-of-plane Π bend			(B_1 state No. 1)	
ν		81.5		81.6	
A		3539.1		3655.4	
B		1737.1		1738.8	
C		1152.3		1172.2	
	$v_{HF}=1$, ground state			(A_1 state No. 1)	
A	3578.3	3593.6	−15.3	3576.9	1.4
B	1742.7	1743.2	−0.5	1745.5	−2.8
C	1162.9	1162.2	0.7	1166.8	−3.9
	$v_{HF}=1$, Σ bend			(A_1 state No. 10)	
ν				79.5	
A				3396.9	
B				1747.7	
C				1170.9	
	$v_{HF}=1$[d]			(B_2 state No. 3)	
ν				61.1	
A				3452.1	
B				1736.5	
C				1135.4	
	$v_{HF}=1$, in-plane Π bend[e]			(B_2 state No. 4)	
ν	62.4	62.0	0.4	62.2	0.2
A	3380.8	3662.9	−281.1	3375.7	5.1
B	1733.4	1715.2	18.2	1743.2	−9.8
C	1120.5	1155.8	−35.3	1125.7	−5.2
	$v_{HF}=1$, out-of-plane Π bend			(B_1 state No. 1)	
ν	88.6	87.6	1.0	87.7	0.9
A	3702.2	3541.4	160.8	3678.8	23.4
B	1754.4	1737.2	17.2	1774.9	−20.5
C	1154.4	1152.8	1.6	1171.8	−17.4

[a]Experimental values taken from Ref. 13.
[b]Reference 14.
[c]This work.
[d]State strongly mixed with in-plane Π bend.
[e]Strongly mixed with framework mode.

portant, the present results are hardly any better than EH. However, when there is a big discrepancy between EH and experiment, the present calculations show much better agreement. In particular, the two largest discrepancies in the earlier work, for the *A* rotational constants of the in-plane and out-of-plane Π bends, are dramatically reduced in the present work.

We have performed limited variations of the energy cutoffs and the basis set (while also investigating convergence of our vibrational results) and conclude that the computed rotational constants should be accurate to better than 30 MHz.

HF bending states have also been observed in the near-infrared spectra of Ar_2HF in the $v_{HF}=3$ state by Klemperer *et al.*[15] We have extended our calculations to model these states. However, for these states the potential energy surface is less accurate and the comparison between theory and experiment is not such a direct test of the computational method. The different issues raised by the rather higher excitation in the HF intramolecular mode will be discussed in a separate paper.[43]

V. CONCLUSION

The vibrational spectrum of the Ar_2HF van der Waals trimer has been investigated up to about 100 cm^{-1} above the zero-point energy for $v_{HF}=0$ and 1. The reported energy levels are converged to an absolute energy of better than 0.1 cm^{-1}. The present method treats fully the van der Waals stretches and therefore gives a density of states much higher than tackled previously for this system. This makes yet better convergence somewhat difficult to achieve. However, we are able to estimate rotational constants of the HF bending vibrational states from $J=1$ levels, because the relative positions of rotational levels converge considerably faster than the absolute energies. This is demonstrated by good agreement between the calculated and experimental rotational constants. The potential of Ernesti and Hutson is successful in reproducing accurately rotational as well as vibrational spectroscopic data.

It is not yet clear how successful our simple strategy is in dealing with states that sample geometries around $R=0$. It seems likely that states similar to the horseshoe states in H_3^+ and Ar_3 do exist in Ar_2HF. Indications of them can be seen in the excited states of Fig. 3. Calculations on states that probe linear geometries are interesting because they might facilitate the observation of such states, and this would allow further improvement of our understanding of nonadditive intermolecular forces. We plan to investigate this further in future work.

The calculations reported here are not very demanding in terms of modern computer power and the results are very encouraging. Applications to many floppy tetra-atomic systems are envisaged including other Rg_2HX clusters. Moreover the extension of our method and program suite to systems of two rare gas atoms and a rigid triatomic molecule such as CO_2 or OCS is not only straightforward but feasible.

ACKNOWLEDGMENTS

The authors are grateful to Mirjana Mladenović, Andreas Ernesti, William Klemperer, Anne McCoy, and Christoph Iung for very useful discussions. This work was funded by the UK Engineering and Physical Sciences Research Council as the ''flagship'' project of CCP6 (the Collaborative Computational Project on Molecular Quantum Dynamics).

[1] X. Chapuisat and C. Iung, Phys. Rev. A **45**, 6217 (1992).
[2] A. R. Cooper and J. M. Hutson, J. Chem. Phys. **98**, 5337 (1993).
[3] D. W. Schwenke, J. Phys. Chem. **100**, 2868 (1996); **100**, 18884 (1996).
[4] *Rovibrational Bound States in Polyatomic Molecules*, edited by M. M. Law, I. A. Atkinson, and J. M. Hutson (CCP6, Daresbury, 1999).
[5] M. Mladenović, J. Chem. Phys. **112**, 1070 (2000).
[6] J. Koput, S. Carter, and N. C. Handy, J. Chem. Phys. **115**, 8345 (2001).
[7] H.-S. Lee and A. B. McCoy, J. Chem. Phys. **116**, 9677 (2002).
[8] *Wide-Amplitude Rovibrational Bound States in Polyatomic Molecules*, edited by I. N. Kozin, M. M. Law, and J. N. L. Connor (CCP6, Daresbury, 2002).
[9] A. McIlroy, R. Lascola, C. M. Lovejoy, and D. J. Nesbitt, J. Phys. Chem. **95**, 2636 (1991).
[10] M. M. Szczęśniak, G. Chałasinski, and P. Piecuch, J. Chem. Phys. **99**, 6732 (1993).
[11] S. M. Cybulski, M. M. Szczęśniak, and G. Chałasinski, J. Chem. Phys. **101**, 10708 (1994).
[12] A. Ernesti and J. M. Hutson, Phys. Rev. A **51**, 239 (1995).
[13] J. T. Farrell, Jr. and D. J. Nesbitt, J. Chem. Phys. **105**, 9421 (1996).
[14] A. Ernesti and J. M. Hutson, J. Chem. Phys. **106**, 6288 (1997).
[15] Ch.-Ch. Chuang, S. N. Tsang, J. G. Hanson, W. Klemperer, and H.-Ch. Chang, J. Chem. Phys. **107**, 7041 (1997).
[16] R. Moszynski, P. E. S. Wormer, T. G. A. Heijmen, and A. van der Avoird, J. Chem. Phys. **108**, 579 (1998).
[17] R. A. Aziz, J. Chem. Phys. **99**, 4518 (1993).
[18] J. M. Hutson, J. Chem. Phys. **96**, 6752 (1992).
[19] H. S. Gutowsky, T. D. Klots, C. Chuang, C. A. Schmuttenmaer, and T. Emilsson, J. Chem. Phys. **86**, 569 (1987).
[20] J. T. Farrell, S. Davis, and D. J. Nesbitt, J. Chem. Phys. **103**, 2395 (1995).
[21] M. J. Elrod, R. J. Saykally, A. R. Cooper, and J. M. Hutson, Mol. Phys. **81**, 579 (1994).
[22] A. Ernesti and J. M. Hutson, Faraday Discuss. Chem. Soc. **97**, 119 (1994).
[23] A. Ernesti and J. M. Hutson, Faraday Discuss. Chem. Soc. **97**, 205 (1994).
[24] J. M. Hutson, S. Liu, J. W. Moskowitz, and Z. Bačić, J. Chem. Phys. **111**, 8378 (1999).
[25] M. I. Hernandez, N. Halberstadt, W. D. Sands, and K. C. Janda, J. Chem. Phys. **113**, 7252 (2000).
[26] F. Gatti, C. Iung, M. Menou, Y. Justum, A. Nauts, and X. Chapuisat, J. Chem. Phys. **108**, 8804 (1998).
[27] C. Iung, F. Gatti, A. Viel, and X. Chapuisat, Phys. Chem. Chem. Phys. **1**, 3377 (1999).
[28] J. Tennyson and A. van der Avoird, J. Chem. Phys. **77**, 5664 (1982).
[29] J. C. Light and T. Carrington, Jr., Adv. Chem. Phys. **114**, 263 (2000).
[30] J. Tennyson and B. T. Sutcliffe, J. Mol. Spectrosc. **101**, 71 (1983).
[31] I. N. Kozin, M. M. Law, J. Tennyson, and J. M. Hutson (unpublished).
[32] J. C. Light, I. P. Hamilton, and J. V. Lill, J. Chem. Phys. **82**, 1400 (1985).
[33] J. Tennyson, J. R. Henderson, and N. G. Fulton, Comput. Phys. Commun. **86**, 175 (1995).
[34] J. Tennyson and B. T. Sutcliffe, J. Chem. Phys. **77**, 4061 (1982).
[35] X. T. Wu and E. F. Hayes, J. Chem. Phys. **107**, 2705 (1997); P. P. Korambath, X. T. Wu, E. F. Hayes, C. C. Carter, and T. A. Miller, *ibid.* **107**, 3460 (1997).
[36] J. R. Driscoll and D. M. Healy, Jr., Adv. Appl. Math. **15**, 202 (1994).
[37] J. R. Henderson and J. Tennyson, and B. T. Sutcliffe, J. Chem. Phys. **98**, 7191 (1993).
[38] M. J. Bramley, J. W. Tromp, T. Carrington, Jr., and G. C. Corey, J. Chem. Phys. **100**, 6175 (1994).
[39] N. J. Wright and J. M. Hutson, J. Chem. Phys. **110**, 902 (1999).
[40] V. A. Mandelshtam and H. S. Taylor, J. Chem. Soc., Faraday Trans. **93**, 847 (1997).
[41] C. R. Le Sueur, J. R. Henderson, and J. Tennyson, Chem. Phys. Lett. **206**, 429 (1993).
[42] G. García de Polavieja, N. Fulton, and J. Tennyson, Mol. Phys. **83**, 361 (1994).
[43] I. N. Kozin, M. M. Law, J. M. Hutson, and J. Tennyson (unpublished).